THE ASTROPHYSICAL JOURNAL, 257:361–372, 1982 June 1

SPECTROSCOPIC EVIDENCE FOR UNDIFFERENTIATED S-TYPE ASTEROIDS

MICHAEL A. FEIERBERG AND HAROLD P. LARSON
Lunar and Planetary Laboratory, University of Arizona
AND
CLARK R. CHAPMAN
Planetary Science Institute, Tucson
Received 1981 April 6; accepted 1981 December 3

ABSTRACT

High-resolution Fourier spectra (0.9–2.5 μm) have been obtained for S-type asteroids 3 Juno, 5 Astraea, 7 Iris, 8 Flora, 9 Metis, 12 Victoria, 18 Melpomene, 27 Euterpe, 29 Amphitrite, 39 Laetitia, and 433 Eros. These data are combined with 0.3–1.1 μm spectrophotometry for compositional analysis. All 11 spectra show olivine and pyroxene absorption features, with olivine/pyroxene abundance ratios between 1 and 10. The range of silicate compositions observed in these asteroids overlaps with the compositions of ordinary and carbonaceous chondrites but does not approach the compositions of the most common differentiated meteorites (pallasites, mesosiderites, and basaltic achondrites). The normalized 2.2 μm reflectances of these asteroids are between 1.2 and 1.7, a reddening that implies the presence of metallic iron. Laboratory spectra of metal-silicate mixtures show that the infrared spectra of the asteroids are compatible with a wide range of metal abundances, but if the metal is finely divided its abundance could be less than 20% by weight. In general, S-type asteroids have spectral reflectances consistent with undifferentiated compositions, and some of them may be ordinary chondrite parent bodies.

Subject headings: abundances — asteroids — infrared: spectra — laboratory spectra

I. THE METEORITE-ASTEROID CONNECTION

Petrological and geochemical investigations of meteorites suggest that they were formed in bodies ranging from 10 to 500 km in diameter (Anders 1964). Upon combining this meteoritic evidence with astronomical observations, an interpretive framework has been developed in which the small solar system bodies broadly defined as asteroids are considered the parent bodies for most or all meteorites (Wasson and Wetherill 1979). This association requires that the compositional differences between the various classes of meteorites be convincingly related to the observed compositions of asteroids. Meteorites can be divided into two basic groups, differentiated and undifferentiated, as a consequence of the thermal histories of their parent bodies. Figure 1 illustrates the compositional structure of idealized parent body sources for these two meteorite groups on the assumption that the terrestrial meteorite flux is derived from collisional fragmentation of such bodies.

Ordinary chondrites are the most common meteorites, accounting for 75% of all observed falls. They are undifferentiated assemblages of solar nebula condensates which may represent the primitive material out of which some of the inner planets formed. Their bulk compositions contain the major nonvolatile elements in amounts close to their cosmic abundances. All ordinary chondrites consist of finely intermixed grains of olivine, pyroxene, feldspar, and metallic Fe, and their parent bodies should be homogeneous, as indicated in the model on the left in Figure 1. Many of the ordinary chondrites have been subjected to some metamorphism within their parent bodies, but none have been melted.

Differentiated meteorites, on the other hand, are derived from parent bodies of initially chondritic composition which experienced at least partial melting soon after formation, resulting in gravitational separation of minerals according to density. The heat sources for these early melting events were probably radioactive decay of

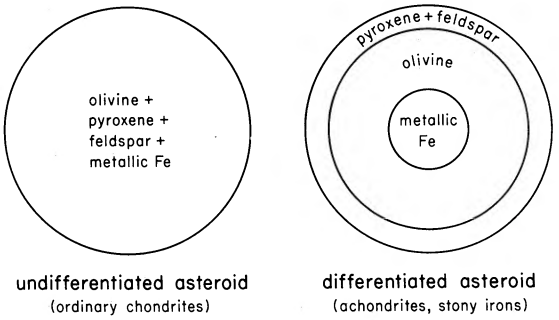

FIG. 1.—Cross sections of idealized meteorite parent bodies. Ordinary chondrites are derived from undifferentiated asteroids and contain finely intermixed grains of olivine, pyroxene, feldspar, and metallic Fe. Differentiated asteroids are formed when a body of initially chondritic composition is melted and there is gravitational separation of minerals according to density. The different types of differentiated meteorites can be understood in terms of depth of formation in their parent bodies. The present asteroid population may consist of fragments of bodies such as these.

short-lived radioisotopes and/or electrical induction by a T Tauri phase solar wind (Sonett and Reynolds 1979). The model on the right in Figure 1 indicates the expected compositional differences between the crust, mantle, and core of a geochemically differentiated asteroid. Melting of a chondritic assemblage at the low pressures characteristic of asteroid interiors produces a pyroxene-plagioclase differentiate and an olivine-rich residue (Walker, Stolper, and Hays 1979). The different types of differentiated meteorites can be understood in terms of depth of formation in their parent bodies. Basaltic achondrites are pyroxene-feldspar igneous rocks erupted onto the surface of their parent body from magma chambers in an olivine-rich mantle (Drake 1979). Pallasites are stony-irons that consist of olivine crystals set in a metallic iron matrix and are apparently derived from the core-mantle boundary of their parent body. Mesosiderites are breccias of iron and silicates; their silicate portions are similar to basaltic achondrites in composition, although the depth of formation in their parent body is not understood. Finally, most types of iron meteorites are probably samples of the cores of differentiated asteroids. Differentiated meteorites containing both olivine and pyroxene are rare, as would be expected from a parent body like the idealized model on the right of Figure 1. In this simple model, all the pyroxene is in the crust and all the olivine is in the mantle, so fragments containing both olivine and pyroxene could not be volumetrically abundant.

On the assumption that the present population of asteroids includes many fragments of parent bodies such as those idealized in Figure 1, compositional information derived from astronomical observations should, in principle, be capable of distinguishing between differentiated and undifferentiated assemblages. That is, fragments of fully differentiated parent bodies should be either olivine-free or pyroxene-free and feldspar-free fragments, and may be either metal-free or metal-rich fragments. Fragments of undifferentiated bodies, however, should contain all four of these minerals.

In this paper, we investigate the compositional relationship between S-type asteroids and the common types of differentiated and undifferentiated meteorites. Our conclusions, which differ from previous interpretive work, bear directly on fundamental questions concerning the origin of meteorites and the processes affecting small bodies in the early solar system.

II. PREVIOUS INTERPRETATIONS OF THE SPECTRAL REFLECTANCES OF S-TYPE ASTEROIDS

On the basis of broadly defined optical properties, 90% of all asteroids can be classified into two distinct groups (Chapman, Morrison, and Zellner 1975; Zellner 1979). Those designated as "C-type" have low albedos (typically 0.04) and neutral colors in the visible part of the spectrum. "S-types" have high albedos (typically 0.15) and reddish colors in the visible region. On plots of color versus albedo, there is a significant gap between members of these two groups. This strongly implies that these two asteroid types are compositionally distinct and have different origins. The colors and albedos of S-type asteroids are superficially like those of meteorites containing silicates and metallic iron, such as ordinary chondrites and stony-irons. C-type asteroids, on the other hand, resemble dark meteorites such as carbonaceous chondrites. Near the inner edge of the asteroid belt S-types are the most numerous, but further out C-types predominate.

The largest observational data set available for compositional analysis of asteroids is the narrow-band spectrophotometry in the 0.3–1.1 μm region presented by Chapman and Gaffey (1979). The average spectrum of an S-type asteroid in this spectral region can be described as follows: a linear, reddened slope from 0.3 to 0.7 μm, a plateau from 0.7 to 0.8 μm, and a shallow absorption feature centered near 1 μm. This spectral reflectance has been interpreted by Gaffey and McCord (1978) as an assemblage containing both metallic Fe and silicates bearing Fe^{2+}. Metallic Fe has a linear, reddened spectral reflectance in the visible and near-infrared regions and appears to dominate the spectra of S-type asteroids. The Fe^{2+}-bearing silicates olivine and pyroxene are the principal components of ordinary chondrites and the silicate portions of stony-irons. These silicate minerals have diagnostic absorption features in the 0.3–2.5 μm spectral region due to Fe^{2+} cations located in different crystal lattice sites. In particular, the 1 μm absorption feature in S-type spectra can be assigned to olivine and/or pyroxene whose compositions are similar to those in ordinary chondrites and stony-irons. The spectrophotometric data also clearly show that there are significant variations in the relative proportions of olivine and pyroxene present on S-type asteroids.

The reflectance spectra of ordinary chondrites have an obvious curvature shortward of 0.5 μm due to an intense silicate absorption in the ultraviolet. This feature is partially suppressed in the spectra of S-type asteroids, whose spectra are more nearly linear between 0.3 and 0.7 μm. This difference has been explained by invoking a higher (50%) metal abundance on S-type asteroids than that found in ordinary chondrites (5%–20%) (Pieters *et al.* 1976). The effect of this opaque, spectrally featureless metal phase would be to suppress the stronger silicate features. The interpretation of S-type asteroids as metal rich was supported by the broad-band *JHK* photometry of Veeder, Matson, and Smith (1978). They found that the normalized 2.2 μm reflectances of S-type asteroids were between 1.3 and 1.8 (normalized to 0.56 μm), clearly much higher than the values between 1.0 and 1.1 measured for ordinary chondrites by Gaffey (1976). These high infrared reflectances were consistent with the high metal abundances inferred from spectrophotometry at shorter wavelengths.

On the basis of the evidence outlined above, the spectral characteristics of S-type asteroids clearly imply a metal-silicate mixture. The "canonical" interpretation is that the present surfaces of these asteroids reveal the iron-rich cores of differentiated parent bodies (Fig. 1, *right*) whose outer silicate crusts have been stripped away by collisions (Chapman 1976). Differentiated stony-iron

meteorites, which account for only 2% of observed falls, would be their meteoritic analogs. However, this association created the problem of there being few, if any, asteroidal parent bodies for the most common meteorite type, the ordinary chondrites. It also conflicts with some inferences from meteoritical studies that ordinary chondrites are a common type of material in the asteroid belt (Anders 1978). Many investigators have suggested that S-type asteroids are in fact ordinary chondrites (i.e., undifferentiated), and that some physical process has enhanced the apparent spectral abundance of metal on their surfaces. The metal abundance on S-type asteroids is difficult to determine since metallic Fe has no diagnostic absorption features and the optical properties of metal-silicate mixtures are not well understood. In addition, the silicate compositions of S-type asteroids have been characterized only approximately from 0.3 to 1.1 μm spectrophotometry since some diagnostic absorption features, particularly those giving the pyroxene composition and the olivine/pyroxene ratio, are located between 1.1 and 2.5 μm. Thus, spectral data farther into the infrared will permit better determinations of the silicate compositions and allow reconsideration of the classification of S-type asteroids differentiated bodies.

In this paper we present high-resolution spectra of 11 S-type asteroids in the 0.9–2.5 μm spectral region. These data are interpreted in combination with the most recent 0.3–1.1 μm spectrophotometry. From the composite spectra, we determine in § III that these S-type asteroids have silicate compositions consistent with undifferentiated meteorites. We demonstrate in § IV that the spectral properties of our limited sample of 11 asteroids are representative of the range observed in classified S-types, although not all extremes are covered. In § V we present laboratory spectra of iron-silicate mixtures that suggest that high metal abundances are not absolutely necessary to explain the observed spectra of S-type asteroids. Finally, in § VI we discuss the compatibility of our new spectroscopic evidence with the parent-body models in Figure 1.

III. DETERMINATION OF SILICATE COMPOSITIONS FROM NEW INFRARED SPECTRA

The spectral reflectances of 11 S-type asteroids observed over the 0.3–2.5 μm region are presented in Figure 2. The 0.3–1.1 μm spectrophotometry is from Chapman and Gaffey (1979). The 0.9–2.5 μm spectra were measured with a Fourier spectrometer (Larson and Fink 1975) operating at a resolution of 50 cm^{-1}. The data for 433 Eros were previously presented by Larson *et al.* (1976). The other 10 spectra were recorded between 1978 September and 1980 October at the 1.5 m telescopes of the University of Arizona Observatories on Mount Lemmon. The Fourier spectra were normalized to 0.56 μm by overlapping them with the spectrophotometry in the region from 0.9 to 1.0 μm. The error bars in the spectrophotometry represent plus or minus 1 standard deviation. In a Fourier spectrum, the average peak-to-peak noise across the spectrum corresponds to approximately three standard deviations.

To derive relative reflectance curves from Fourier spectra, the observed spectra of the asteroids are divided by the spectra of comparison stars with spectral types ranging from F7 V to G7 V. In all cases, the comparison stars were observed within 45 minutes and 0.03 air mass of the asteroid observations. Most of our spectra are averages of several sets of asteroid-comparison star observations recorded on consecutive nights. The colors of the comparison stars were independently confirmed by broad-band JHK photometry (Lebofsky 1980). Our measurements agree with the finding of Low and Rieke (1974) that stars in this spectral range have a spread of about 0.10 in their $J-K$ color indices. The small differences between the colors of our comparison stars and that of the Sun are removed from our data by applying linear corrections to the slopes of the asteroids' relative reflectance curves.

The 11 asteroids observed with the Fourier spectrometer are among the brightest visible from the Earth, having K-magnitudes (2.2 μm) less than 9 at the time of our observations. The asteroid 433 Eros is an Earth-approacher with a diameter of 20 km. The other 10 are located in the inner half of the main belt and have diameters between 110 and 250 km. The extent to which this small sample is representative of the general population of S-type asteroids will be discussed in detail in § IV.

The infrared spectrum (0.7–2.5 μm) of the typical S-type asteroid is described as follows: an absorption feature centered near 0.95 μm, a weaker absorption feature centered around 1.9–2.0 μm, a maximum between these two absorptions at 1.5–1.6 μm, and an overall reddened slope. The normalized 2.2 μm reflectance of the spectra in Figure 2 fall between 1.21 and 1.74. This is in agreement with the previously cited broad-band JHK photometry of Veeder, Matson, and Smith (1977) for the 9 of our 11 asteroids that they measured. In 6 of the 9 cases, the 2.2 μm reflectances agree within a few percent; in the other 3 cases, there is agreement within the combined uncertainties.

The spectra contained in Figure 3 illustrate the basis of our silicate analysis. The infrared spectra (0.7–2.5 μm) of asteroids 8 Flora, 27 Euterpe, and 9 Metis are included as examples of S-type asteroids whose spectra share the characteristics described above, but whose absorption features show significant differences. The slope of the apparent continuum level in each spectrum was removed to permit more direct comparisons of their Fe^{2+} silicate features with those in the spectra of terrestrial and meteoritic minerals. We assumed that the continuum level is linear in wavenumber, piecewise continuous, and tangent to the spectral reflectance curve outside the silicate absorptions.

Figure 3 also contains representative laboratory comparison spectra of three meteoritic silicates: olivine, pyroxene, and feldspar. Only the pyroxene displays an absorption near 2 μm. Thus, the features near 0.95 and 2.0 μm in the asteroid spectra can be uniquely assigned

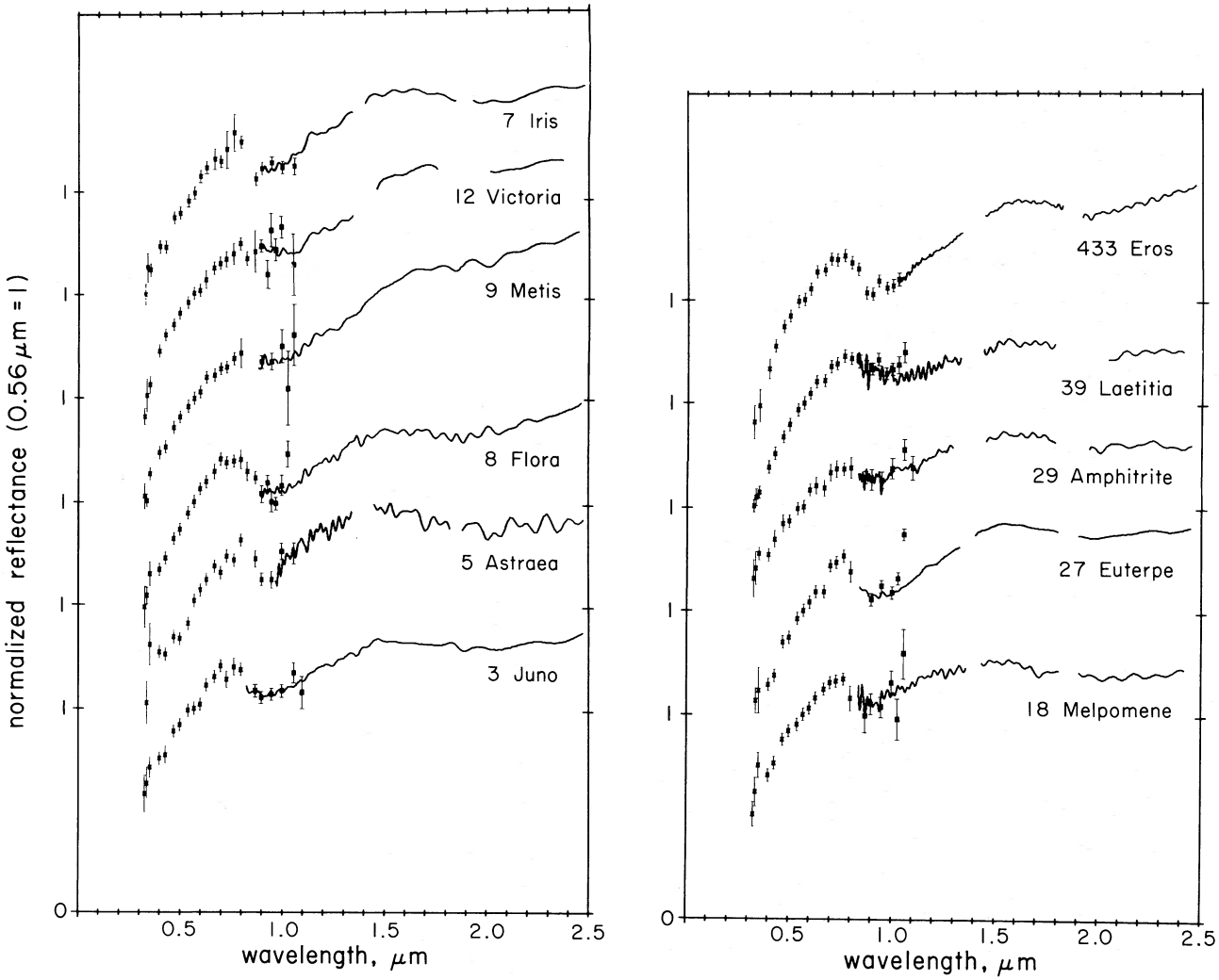

FIG. 2.—The spectral reflectances of 11 S-type asteroids observed over the 0.3–2.5 μm region. The 0.3–1.1 μm spectrophotometry is from Chapman and Gaffey (1979). The 0.9–2.5 μm Fourier spectrum of 433 Eros is from Larson *et al.* (1976). The other Fourier spectra are presented here for the first time. The spectrophotometry is normalized to unity at 0.56 μm, and the infrared spectra are normalized to the filter data between 0.9 and 1.0 μm. The vertical scale is the same for each spectrum, but the zero points are indicated only for the lower spectrum in each group.

to a pyroxene component. However, the 0.95 μm asteroid features are significantly stronger than those at 2 μm, and they extend asymmetrically to longer wavelengths. This implies the presence of another mineral which absorbs primarily in the 1 μm region. Both olivine and feldspar have broad absorptions near 1 μm that extend beyond 1.5 μm, but Figure 3 demonstrates that their spectral behavior when mixed with pyroxene is quite different, thus permitting a distinction between olivine-pyroxene and pyroxene-feldspar mixtures. The spectrum of a type L chondrite (Fig. 3, *center*) illustrates a mixture of olivine and pyroxene whose spectral characteristics are clearly influenced by both components. The 0.9 μm pyroxene band and the 1.1 μm olivine band are blended, producing an asymmetrically broadened band centered at 0.95 μm. The strength of the 2 μm band has been decreased relative to that of the 1 μm band because the abundance of pyroxene is less and olivine has no 2 μm band. These changes in the 1 and 2 μm bands cause the position of the maximum between the bands to shift to a longer wavelength. The spectrum of the eucrite (Fig. 3, *right*) illustrates the spectral characteristics of a mixture of pyroxene and feldspar. The blending of the 0.9 μm pyroxene band and the 1.2 μm feldspar band also has the effect of shifting the position of the maximum to longer wavelengths. However, there is little change in the relative strength of the two pyroxene bands because the Fe^{2+} absorption in feldspar is extremely weak at 0.9 μm. In the spectra of the S-type asteroids (Fig. 3, *left*), the 2 μm bands are clearly weakened relative to the 1 μm bands. On this basis we conclude that the spectra of S-type asteroids contain blended olivine and pyroxene absorptions, as in the spectrum of the L chondrite.

To put our analysis on a quantitative basis, we made

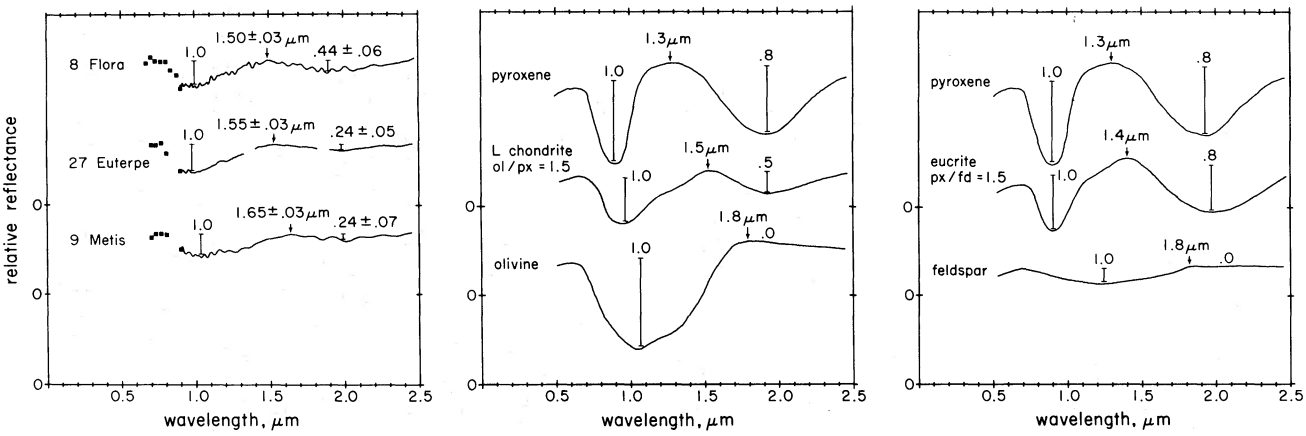

FIG. 3.—The 0.7–2.5 μm spectra of three representative S-type asteroids and comparison spectra of meteoritic silicates. These spectra illustrate the basis of our silicate analysis. The ratio of the depths of the absorption bands (2 μm/1 μm) and the position of the maximum reflectance between the bands are spectral parameters dependent upon the relative abundances of olivine, pyroxene, and feldspar. The spectra of S-type asteroids clearly contain blended olivine and pyroxene absorption bands.

the following measurements from the spectral reflectance curves, as indicated in Figure 3: (1) the strength of the 2 μm band relative to that of the 1 μm band and (2) the position of the local maximum in the spectral reflectance between these bands. We used these two parameters to infer the silicate compositions of our S-type asteroids. The dependence of these parameters on composition was established by measuring the reflectance spectra of properly prepared samples of known composition. This has been done for meteorites by Gaffey (1976) and for terrestrial minerals by Singer (1981). A calibration derived from their results is presented in Figure 4.

Figure 4 compares the position of maximum reflectance between bands to band depth ratio for the 11 asteroids in this study. Pure olivine and pure pyroxene with compositions similar to those in ordinary chondrites and stony-irons plot in the upper right and lower left, respectively, as indicated by the circles in Figure 4. Mixtures of olivine and pyroxene plot along the dashed line connecting the two points, shifting toward the upper

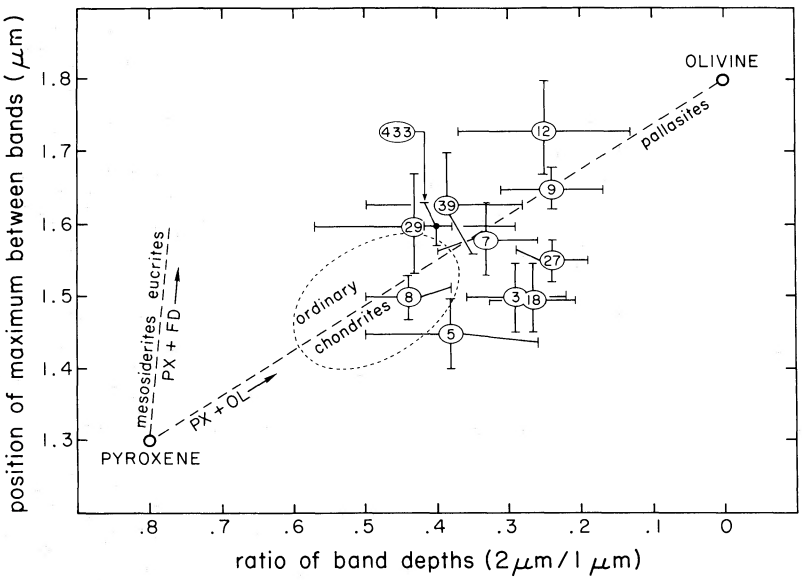

FIG. 4.—A plot of the composition-dependent spectral parameters (illustrated in Fig. 3) for all 11 S-type asteroids in our study. The positions of common meteoritic silicate assemblages are labeled. The dashed oval encloses the range of known ordinary chondrites. All the asteroids plot along the olivine-pyroxene line, proving that they contain substantial amounts of olivine and pyroxene. The asteroid 8 Flora has an olivine/pyroxene ratio of about 1–2, indistinguishable from that of ordinary chondrites. The asteroid 9 Metis may have an olivine/pyroxene ratio as high as 5–10, similar to that of carbonaceous chondrites. None of the asteroids plot near the points for pure olivine or for pyroxene plus feldspar. Thus, the silicate compositions of S-type asteroids are like those of chondritic meteorites and do not resemble those of differentiated meteorites.

right with increasing olivine content. Mixtures of pyroxene and feldspar plot along the dashed line on the left side, shifting toward the upper left with increasing feldspar content. The locations of the various meteorite types are also marked in Figure 4. All ordinary chondrites cluster tightly around a maximum position of 1.5 μm and a band depth ratio of 0.5. Their olivine/pyroxene ratios fall in a narrow range between 1 and 2. Differentiated meteorites, on the other hand, have a distinct bimodal distribution on this plot. Pallasites, whose silicate fractions are almost entirely olivine, cluster tightly around the point for pure olivine at a maximum position of 1.8 μm and a band depth ratio of 0 (no 2 μm band). Mesosiderites and eucrites, whose silicate components are almost entirely pyroxene and feldspar, plot along the left side of the graph with maximum positions around 1.4–1.5 μm and a band depth ratio of 0.8. There are no meteorites containing more than about 50% feldspar, so the pyroxene-feldspar line terminates at the position of eucrites. Very few differentiated meteorites have silicate compositions whose spectral parameters plot midway along the olivine-pyroxene line. No known ordinary chondrites have silicate compositions which would plot near the extremes of the olivine-pyroxene line. Thus, known primitive and differentiated meteorites are clearly separated on this plot on the basis of the spectral parameters dependent upon their silicate components.

Following the examples in Figure 3, we have plotted on Figure 4 the values of these two parameters for the 11 S-type asteroids in our study. The error bars have been estimated subjectively but are expected to correspond to about plus or minus 1 standard deviation. The error bars for the band depth ratios tend to be large because of the weakness of the 2 μm bands and the fact that the 2 μm bands are partially obscured by telluric H_2O absorption at 1.9 μm. The error bars for the positions of the maxima are small because the Fourier spectra have their highest signal-to-noise ratios at 1.6 μm, exactly where the maxima occur. It is possible that there could be a systematic shift in the asteroid parameters relative to those of the meteorite samples due to the presence of metallic iron on the asteroids. The metal would probably reduce the depths of the 2 μm bands relative to those of the 1 μm bands (Pieters *et al.* 1976), thus shifting the asteroid data points toward the upper right in Figure 4. This shift would make the asteroids appear more olivine rich than they actually are. We can make no quantitative estimate of the size of this effect, but we feel that it is probably small compared to the observational uncertainties.

The asteroid data cluster about midway along the olivine-pyroxene line, proving that substantial amounts of olivine and pyroxene are present. Those asteroids plotting toward the lower left, such as 8 Flora, have olivine/pyroxene ratios of 1 or 2, overlapping the range of ordinary chondrites. Those in the upper right, such as 9 Metis, have higher olivine/pyroxene ratios, with values as high as 5 or 10 possible. Olivine-rich meteorites containing less than 10% pyroxene do not show 2 μm absorptions in their spectra (Gaffey 1976), so any olivine/pyroxene ratios higher than 10 would be inconsistent with the presence of 2 μm features in all the asteroid spectra in Figure 2. Thus, the silicate compositions of the 11 S-type asteroids in our study range from 50% to 90% olivine and 10% to 50% pyroxene. The inferred olivine/pyroxene ratios for a majority of the asteroids in Figure 4 are higher than that of ordinary chondrites. Type CV and CO carbonaceous chondrites have olivine/pyroxene ratios typically around 10, although they have never been seriously considered as being possible meteoritic analogs for S-type asteroids. This is because carbonaceous chondrites contain low-albedo opaques such as carbon and magnetite, which lower their albedos below those of S-type asteroids and substantially mask their silicate absorption features. Also, they lack the metallic iron that appears to be responsible for the reddening of the asteroid spectra. It is especially significant that none of the 11 asteroids have spectral parameters that plot in Figure 4 near the values for pure olivine or pure pyroxene, or for pyroxene-feldspar mixtures.

For the asteroids with higher quality infrared spectra in Figure 3, we can also determine the compositions of their pyroxenes. As stated earlier, the 2 μm absorption bands are uniquely assigned to Fe^{2+} cations in pyroxene, and these bands shift to longer wavelengths with increasing Fe end-member abundance. Thus, using calibrations by Adams (1974) for orthopyroxenes and low-calcium clinopyroxenes, the observed 2 μm band position directly gives pyroxene composition. When combined with the olivine/pyroxene ratios determined above, an additional criterion becomes available to help distinguish between primitive and differentiated assemblages. We have determined that 8 Flora has one of the lowest olivine/pyroxene ratios (1–2) in our sample, and its 2 μm band position of 1.90 ± 0.03 μm is consistent with a pyroxene composition like that in ordinary chondrites, between Fs_{16} and Fs_{27}. The asteroid 9 Metis has one of the highest olivine/pyroxene ratios (5–10) in our sample, and the band position of 2.00 ± 0.06 μm indicates a pyroxene composition which is more iron rich than that in ordinary chondrites but is consistent with that of carbonaceous chondrites. The band positions for the other nine asteroids in our study appear to fall between 1.9 and 2.0 μm, but in most cases the uncertainties are too large to permit mineralogical analyses. The observed band positions for ordinary chondrites also range from 1.9 to 2.0 μm (Gaffey 1976), so the pyroxene compositions of the asteroids in our study are consistent with ordinary chondrites. High-calcium pyroxenes like those in some basaltic achondrites (band positions > 2.0 μm) are not observed, although they cannot be ruled out for some of the noisier spectra in Figure 3.

Thus, we conclude that the silicate compositions of these S-type asteroids correspond to those of undifferentiated meteorites. Some of the asteroids have olivine/pyroxene ratios and pyroxene compositions like those of known ordinary chondrites. The others have

silicate compositions like CV and CO carbonaceous chondrites, but with less carbon and magnetite and more metallic Fe. None of the common differentiated meteorite types are plausible meteoritic analogs for these S-type asteroids.

IV. THE DIVERSITY OF S-TYPE ASTEROID SPECTRA

The purpose of this section is to place the 11 S-type asteroids for which composite infrared spectra exist into the context of the larger sample of S-type asteroids observed at wavelengths shortward of 1.1 μm by filter spectrophotometry. Chapman and Gaffey (1979) identified 98 asteroids as having S-type (or S-like) spectra. Forty-six of these were not measured sufficiently far into the infrared to characterize their 1 μm absorption features. The remaining 52 were divided by Chapman and Gaffey into 22 groups with recognizably different spectra.

For the purposes of this paper, we have redefined the groupings using criteria relevant for comparison with the 0.9–2.5 μm Fourier spectra. We are particularly interested in the structure of the near-infrared absorption feature present in spectra of most S-type asteroids between 0.9 and 1.1 μm. Unfortunately, filter data in this wavelength range are rather noisy for most asteroids because of the survey nature of the observing program and the relative insensitivity of detectors. We have, therefore, excluded several especially noisy spectra and used somewhat less restrictive criteria (especially for spectral parameters, such as overall redness, that are not directly related to the absorption band) in regrouping 45 complete filter spectra of good quality.

The groups were assembled largely on the basis of spectral parameters contained in the TRIAD file. For their definitions, see Chapman and Gaffey (1979). Given the number of variables involved and the fact that there do not seem to be distinct clusters of properties, the groupings should be thought of as a division of a continuum of spectra rather than as an identification of well-defined types. Some asteroids (e.g., 3, 17, 30, 532) fall near the boundaries of groups and could have been placed in either of two groups. There is a significant amount of variation within some of the groups in parameters, such as redness and band depth, which are related to spectral contrast.

Table 1 lists our nine modified S-type groups, including the member asteroids, and the means and ranges of eight spectral parameters. Weighted mean spectra for the nine groups are plotted in Figure 5. This comparison clearly reveals the important differences among S-type spectra. We describe below the mineralogical significance of these differences in the 0.3–1.1 μm spectra.

The overall redness of a spectrum in the visible region is measured by R/B or, toward shorter wavelengths, by the $U-B$ and $B-V$ color indices. The redness of S-type spectra is believed to result from Fe^{2+}-bearing silicates (e.g., pyroxene and olivine) as well as metallic Fe. S-type asteroids with less red colors than average may contain some colorless opaque minerals, such as carbon or magnetite. Differences in surface texture and particle size also may modify reddening. The curvature of the visible part of the spectrum is measured by the bend parameter. A straightforward interpretation of differences in bend, for assemblages of metal mixed with iron-bearing silicates, is that large values of bend correlate with smaller quantities of metal.

The chief differences among the nine spectral groups studied concern the 1 μm absorption band: its depth, its position, and its shape. Band depth is affected, in part, by the quantity and particle sizes of the mineral or minerals contributing to the feature. In addition, band

TABLE 1

S-TYPE SPECTRAL GROUPS: PARAMETER MEANS AND RANGES

Group	Member Asteroids[a]	R/B	$U-B$	$B-V$	Bend	IR	Depth	Band Ctr. (μm)	Bandwidth (μm)
A	*12*, 30, 119,	1.63	0.46	0.86	0.11	0.05	1.00	...	...
	196, 236, 1449	1.45–1.77	0.44–0.51	0.84–0.89	0.07–0.15	−0.01–0.08	1.00–1.00		
B	108, 115, 341	1.65	0.47	0.87	0.13	0.27	0.94	0.91	0.12
		1.55–1.75	0.46–0.48	0.85–0.92	0.07–0.18	0.24–0.31	0.91–0.98	0.90–0.92	0.09–0.14
C	*9*, 23, *29*, 40,	1.57	0.44	0.86	0.10	0.10	0.94	0.93	0.13
	79, 89, 230, 674	1.44–1.66	0.42–0.50	0.84–0.88	0.05–0.16	0.07–0.16	0.90–0.98	0.90–0.95	0.09–0.15
D	6, 11, 14, *18*, 20,	1.53	0.40	0.84	0.10	0.01	0.89	0.92	0.17
	32, 37, 82, 532	1.43–1.60	0.36–0.44	0.81–0.86	0.06–0.14	−0.05–0.07	0.86–0.93	0.90–0.94	0.14–0.21
E	63	2.01	0.47	0.91	0.13	0.01	0.90	0.95	0.15
F	*8*, 17, 25,	1.74	0.47	0.88	0.12	0.00	0.85	0.93	0.18
	27, 28	1.63–1.89	0.41–0.51	0.84–0.93	0.07–0.15	−0.06–0.11	0.82–0.89	0.89–0.95	0.15–0.21
G	*39*, 192, 760	1.71	0.50	0.92	0.11	0.01	0.92	0.94	0.19
		1.68–1.75	0.49–0.52	0.89–0.95	0.08–0.13	0.01–0.01	0.90–0.95	0.93–0.96	0.17–0.21
H	*3*, 7, 15, 68	1.58	0.45	0.83	0.08	−0.07	0.90	0.98	0.27
		1.53–1.67	0.42–0.49	0.82–0.84	0.06–0.10	−0.09–(−0.02)	0.88–0.92	0.94–1.02	0.21–0.36
I	43, 116, *433*,	1.67	0.46	0.86	0.15	−0.11	0.85	0.96	0.22
	887, 1055, 1685	1.48–1.75	0.40–0.50	0.82–0.88	0.09–0.19	−0.16–(−0.05)	0.80–0.90	0.93–1.02	0.18–0.30

[a] Italicized asteroids are part of our composite sample.

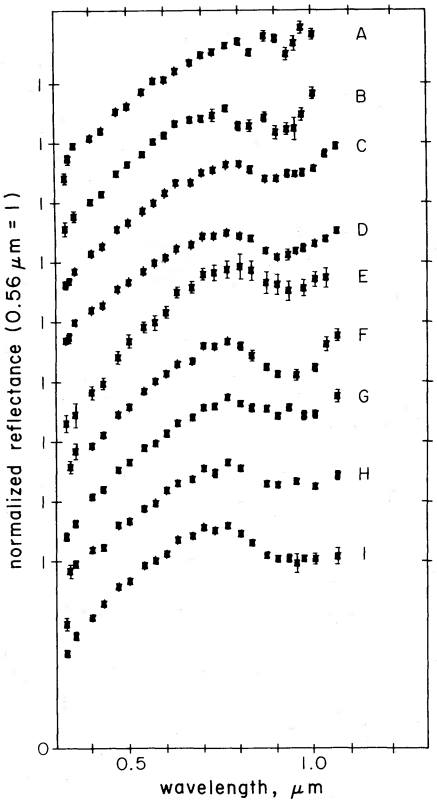

FIG. 5.—The diversity seen in the 0.3–1.1 μm spectrophotometry of 45 S-type asteroids by Chapman and Gaffey (1979). Each curve is the average spectrum of a group of asteroids having similar spectra, especially similar 1 μm absorption features. The 11 asteroids for which 0.3–2.5 μm composite spectra exist cover much of the diversity seen in typical S-type asteroids, so there should be no observational bias in the data in Fig. 4.

depths may be diminished by finely disseminated opaques (either metal or colorless opaques).

The spectral parameters "IR" (infrared slope), band center, and bandwidth all correlate with the relative proportion of pyroxene and olivine as well as with the elemental compositions of the silicates (e.g., fraction of iron, magnesium, or calcium). Orthopyroxene is clearly present on many S-type asteroids, as indicated by absorption bands with center wavelengths shortward of 0.93 μm (Adams 1974). The broadened bands and strongly negative values of the infrared slope parameter (indicating depressed reflectance near 1.05 μm) are indicative of olivine (see Chapman and Salisbury 1973). Greater proportions of olivine are indicated by larger values of the center wavelength and bandwidth parameters and by strongly negative values of the infrared slope parameter. These criteria would be somewhat different if we admitted the possibility that a calcium-rich clinopyroxene were present, but a variety of evidence, including the center wavelengths of all the 2 μm absorption bands observed in the spectra in Figure 2, demonstrates that such clinopyroxenes are not present.

We now describe each group and how each of the 11 asteroids in Figure 2 relates to them. The mineralogical interpretations are based on the 0.3–1.1 μm spectrophotometry only.

Group A spectra lack discernible absorption bands, although they tend to flatten longward of 0.8 μm, which may indicate the minor presence of an iron-bearing silicate such as olivine. These asteroids probably have a larger mixture of opaques and/or colorless silicates than is typical for S-type asteroids. The asteroid 12 Victoria is a member of this group. The infrared filter data for Victoria are rather noisy and are not inconsistent with the suggestion of weak olivine-pyroxene bands in its 0.9–2.5 μm Fourier spectrum in Figure 2.

Group B spectra exhibit a modest orthopyroxene absorption but show no evidence for olivine. None of the 11 asteroids with composite spectra in Figure 2 are represented in this very olivine poor group.

Group C spectra are also dominated by a pyroxene absorption feature, but either the pyroxene is more iron-rich or calcium-rich than in the case of group B or, more likely, there is an admixture of some olivine. Nevertheless, these asteroids appear to be olivine poor in comparison with most S-types. A member of this group, 9 Metis, has a shallower absorption band and is partly like group A asteroids. The asteroid 29 Amphitrite, also a member of group C, is less red and has a smaller bend value than average.

Group D asteroids are also olivine poor. In addition, their spectra are much less red than those of any other group. A typical member of this group is 18 Melpomene. The asteroid 5 Astraea would probably be a member of group D, but its filter data were not included in the average because of their lower quality.

Group E consists of a single asteroid which is unusually reddish and has a rather large bend value. Other parameters have intermediate values.

Group F spectra are also rather red, but their chief feature is an unusually deep absorption band. Both 8 Flora and 27 Euterpe are typical members of this group.

Group G are the reddest spectra. Like group F, they imply intermediate proportions of olivine, but unlike group F the absorption bands have the modest depths typical of S-type asteroids. The spectrum of 39 Laetitia is fairly similar to spectra of the other two members of this group.

Group H asteroids are apparently olivine rich. In addition, this group exhibits the lowest mean value for the bend parameter. The asteroid 7 Iris is a typical member of this group. However, 3 Juno is not a completely typical member of this group. It appears to have an intermediate proportion of olivine, and its spectrum is less red than other spectra in the group. Three of the four asteroids that compose this group are the three largest S-type asteroids in the asteroid belt.

Group I spectra have unusually deep absorption bands. Their bandwidths, band centers, and infrared slope parameters indicate an olivine-rich mixture of silicates. Also, the bend parameter is unusually large, indicating a relatively metal free composition. The asteroid 433 Eros may be a little less olivine rich than

is typical of this group. All of these asteroids are small and many of them are Earth-approachers.

Of the nine S-type spectral groups identified from 0.3–1.1 μm filter data, seven are represented in our 0.3–2.5 μm composite sample. No asteroids in group B, the most olivine poor, or group E, the most reddened, have been observed beyond 1.1 μm. In some individual cases, there are discrepancies between the olivine/pyroxene ratios inferred in this section and those inferred in § III. We estimate that the determinations of the olivine/pyroxene ratios from the 1 μm band shape of the filter data in Figure 5 have typical uncertainties about twice as large as those of the determinations made from the 0.7–2.5 μm spectra in Figure 4. For the noisier spectra, the combined uncertainties of the two methods are equal to the total spread seen in the data in Figure 4, so the differences in inferred olivine/pyroxene ratios are not serious inconsistencies.

The 0.3–1.1 μm filter data appear to show a wider range of olivine/pyroxene ratios than is seen in our sample of 11 in Figure 4. Although part of this spread may be due to uncertainties in the filter data, it is likely that a small percentage of this larger sample of S-types has more extreme olivine/pyroxene ratios than any in our composite sample. It cannot be excluded that a few S-type asteroids have olivine without pyroxene or pyroxene without olivine. However, the asteroids in our 0.3–2.5 μm study cover much of the diversity among typical S-type asteroids, and they all contain significant proportions of both olivine and pyroxene.

V. THE ABUNDANCE OF METALLIC IRON ON S-TYPE ASTEROIDS

In the preceding sections of this paper we have concentrated on the silicate compositions of our sample of S-type asteroids as a criterion for distinguishing between primitive and differentiated mineralogies. This emphasis is partly because olivine and pyroxene have diagnostic spectral features in the infrared which are easily measured and interpreted. However, the abundance of free metallic iron on these asteroids, if it could also be determined accurately, would be an equally important criterion. Clearly, if some future observation (e.g., density) were to demonstrate conclusively that S-type asteroids contain 50% by weight metallic iron, then we would be forced to conclude that they are differentiated objects. Our problem would then be to account for their apparently undifferentiated silicate compositions. At this time, however, we must examine the available spectral data to determine what constraints actually exist on the metal abundances of S-type asteroids.

Previous interpretations have identified S-type asteroids with metal-rich stony-iron meteorites, principally because their reflectance spectra appear to be dominated by metallic iron (Gaffey and McCord 1978). Compared with ordinary chondrites, S-type asteroids have more linear and reddened spectra, shallower silicate absorption features and lower albedos (Zellner 1979). We conducted laboratory studies of iron-silicate mixtures to demonstrate how these spectral characteristics are influenced by metal abundance and distribution. Some of these laboratory spectra are compared with asteroid spectra in Figure 6.

In Figure 6 (*left*) we present first the 0.9–2.5 μm spectra of 8 Flora and 349 Dembowska. Comparison of their spectra is useful because they are both main-belt asteroids of similar size (about 150 km in diameter), and spectral differences between them should be due to real compositional differences rather than differences in surface texture. Dembowska is an unusual R-type asteroid whose reflectance spectrum indicates an olivine-rich, metal-poor composition (McCord and Chapman 1975; Gaffey and McCord 1978; Feierberg *et al.* 1980). The silicate-dependent spectral parameters for Dembowska plot among the S-type asteroids in Figure 4. In other optical parameters, however, Dembowska differs greatly from S-type asteroids. Dembowska has a much higher albedo (0.28) and deeper absorption bands due to its apparent lower abundance of metallic iron. Assuming that 349 Dembowska is a metal-free olivine-pyroxene assemblage, the spectral reflectance of 8 Flora can be modeled with a similar silicate mixture plus an opaque mineral with a lower albedo such as metallic

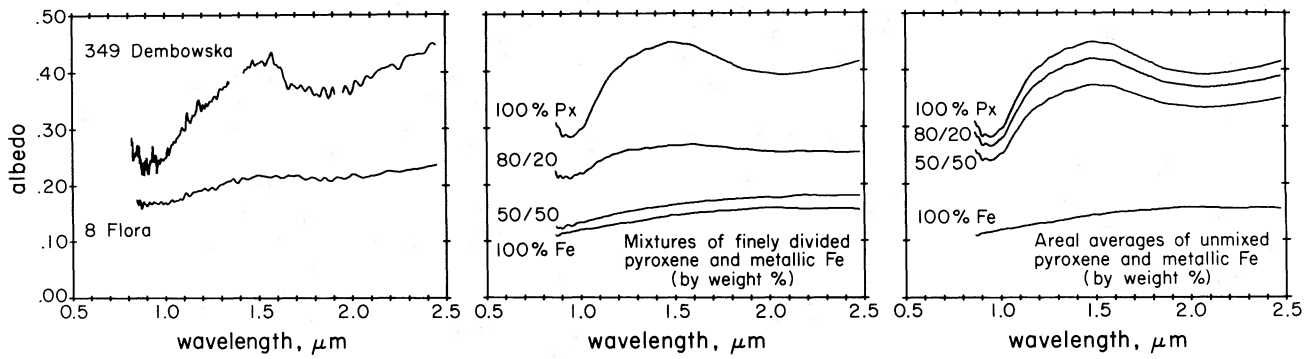

FIG. 6.—The effect of metallic iron on the reflectance of silicates. Asteroid 349 Dembowska has olivine and pyroxene features similar to those of S-type asteroids but is distinguished by its higher albedo and larger band depths. The albedo, band depths, and degree of reddening of 8 Flora are typical of the asteroid spectra in Fig. 2. The amount of metal required to produce the observed spectra of S-type asteroids depends upon the physical state of the metal.

iron. The amount of metal required to produce the difference between Dembowska's and Flora's spectra is very important. If it is 20% by weight or less, the composition of 8 Flora may be indistinguishable from that of ordinary chondrites. If, however, much more than 20% by weight is required, 8 Flora may be better modeled as a differentiated stony-iron object.

In simulations of an asteroid's surface mineralogy it is important to adjust particle size and other textural parameters, especially for opaque components. We have included in Figure 6 laboratory spectra representing two extremes: finely divided iron intimately mixed with the silicates, and isolated macroscopic patches of metal and silicate. To simulate the silicates on asteroids, we prepared a powdered sample of a terrestrial pyroxene with particle sizes less than 74 μm. As shown in Figure 6 (*center*, top spectrum), this sample reproduces the band depth and albedo characteristics of asteroid 349 Dembowska, although the asteroid undoubtedly contains a great deal of olivine in addition. To simulate the metallic iron on asteroids, we used a sample of powdered iron (Fischer Scientific Co.) with particle sizes between 33 and 74 μm. The metallic iron in ordinary chondrites and stony-irons contains a few percent nickel, but this does not substantially affect its color. Most metal grains in ordinary chondrites are larger than 100 μm (Affiatalab and Wasson 1980), but metal grains on asteroid surfaces might be more finely divided. Meteoritic iron is ductile at room temperature, but at temperatures below 200 K, more typical of main-belt asteroids, iron becomes brittle and could be fractured by high-velocity impacts (Remo and Johnson 1974).

In our first experimental simulation, we mixed the pyroxene and metal powders in varying proportions, and measured the infrared reflectance spectra of the samples using the same Fourier spectrometer that was used for the asteroid observations. The results are shown in Figure 6 (*center*). The admixture of 20% by weight of metal produces a substantial reduction in the absolute band depths and albedo of the sample, comparable to the difference between the asteroids 349 Dembowska and 8 Flora. The spectrum of this mixture is not reddened to the same degree as that of Flora because we did not mix any olivine with the pyroxene. The additional reddening in Flora's spectrum is caused by the presence of abundant olivine. The relative strengths of the 1 and 2 μm pyroxene bands remained constant with the admixture of metal, providing evidence that the spectral parameters developed in § III to determine the silicate compositions are largely independent of metal content. Addition of 50% metal almost completely suppresses the pyroxene bands and the sample appears almost indistinguishable from pure metal. If the particle sizes of silicate and metal in our experiments are like those on asteroids, then the infrared spectra of 8 Flora and other S-type asteroids do not require that more than 20% by weight of metal be present. More significantly, an abundance of 50% metal, like that in stony-iron meteorites, could be ruled out.

Our second experimental simulation assumed that S-type asteroids have surfaces that are variegated on a scale of centimeters or kilometers, with separate areas of pure silicate and pure metal. In this case, observations of asteroids would be hemispherical, areal averages of silicate and metal reflectance spectra. In Figure 6 (*right*) we have simulated such a "checkerboard" surface by averaging the spectra of metallic iron and pyroxene according to areal coverage, assuming the density of the metal is 3 times that of the silicate. Assemblages with 20%–50% by weight of metal have spectra which differ very little from pure pyroxene. If 8 Flora has such a variegated surface, it could easily contain 50% or more metallic iron. In fact, 349 Dembowska could also have a lot of metallic iron. From the examples in Figure 6 it is apparent that the physical state of the surface plays a very important role in the relative spectral contribution of metallic iron. Therefore, it is important to be aware that spectral observations alone cannot uniquely constrain the metal abundance on the surfaces of asteroids to any particular value. In particular, there is no quantitative basis for concluding that S-type asteroids have an excess of metallic iron relative to that found in ordinary chondrites.

VI. DISCUSSION

From our analysis of the infrared reflectance spectra of 11 S-type asteroids, we conclude:

1. The silicate compositions of the 11 S-type asteroids in our study resemble those of undifferentiated (chondritic) meteorites in terms of olivine/pyroxene ratios and pyroxene compositions.
2. None of our sample of 11 S-type asteroids have silicate compositions resembling those of any common differentiated stony-iron meteorites (the nearly olivine-free mesosiderites or the nearly pyroxene-free pallasites).
3. Our sample is representative of the spectral diversity of S-type asteroids, although a small percentage of S-types apparently have more extreme olivine/pyroxene ratios.
4. The infrared spectra of S-type asteroids are compatible with a wide range of metallic iron abundances, but values less than 20% by weight are sufficient to match all observational constraints if the metal is very finely divided and uniformly dispersed.

In Figure 1 we presented idealized models of differentiated and undifferentiated asteroids. We now examine the above spectroscopic evidence in combination with the meteoritic evidence to test the compatibility of S-type asteroids with these models.

The conventional interpretation of S-type asteroids is that they are differentiated bodies like the model on the right in Figure 1, with most of the outer silicate layers stripped away. Their surfaces would consist of olivine and metallic iron, corresponding to pallasites (olivine stony-irons) in composition. This prediction is contradicted by our conclusion (1), above, that the 11 S-type asteroids we studied have chondritic proportions of olivine and pyroxene on their surfaces. Therefore, we can rule out the possibility that S-type asteroids resemble the differentiated asteroid model in Figure 1. However,

there are two alternative models for differentiated asteroids which, in some cases, predict chondritic proportions of olivine and pyroxene on their surfaces. These models of S-type asteroids are consistent with our spectroscopic evidence outlined above, but as we show below, are not supported by the meteoritic evidence.

The first alternative model involves differentiated bodies like that in Figure 1 which have been disrupted by collisions. It is almost certain that some asteroids have suffered major collisions over the age of the solar system. In at least a few cases, collisional mixing of the crust and mantle of differentiated bodies should produce regoliths or breccias containing both olivine and pyroxene on their surfaces (Chapman and Greenberg 1981). If S-type asteroids are such bodies, our conclusions (2) and (3), above, would require that nearly all S-type asteroids have been thoroughly mixed by collisions. Since we have no meteorite sample of such mixtures, however, olivine-pyroxene mixtures cannot be common on asteroid surfaces. We therefore believe it is unlikely that many S-type asteroids are differentiated and collisionally remixed bodies.

The second alternative model involves differentiated bodies with a complex differentiation history. In the weak gravitational field of an asteroid, the pyroxene-plagioclase differentiate arising from melting in the interior might not rise all the way to the surface. Likewise, the denser olivine-rich residue left over from melting near the surface might not sink all the way into the mantle. In this way, olivine-rich and pyroxene-rich rocks could be present in close proximity near the surface. If S-type asteroids are such bodies, our conclusion (1), above, would require that the olivine-rich rocks are several times more abundant on their surfaces than the pyroxene-rich differentiates. However, we have approximately 70 samples of pyroxene-plagioclase basaltic achondrites and no meteorite samples of their olivine-rich source material. We therefore believe it is unlikely that many S-type asteroids are heterogeneously differentiated bodies.

The alternative to the above interpretations is that S-type asteroids are undifferentiated bodies like the model on the left in Figure 1. The presence of chondritic abundances of olivine, pyroxene, and metallic iron on all S-type asteroids is consistent with all the spectroscopic evidence summarized above. This interpretation is also supported by some meteoritic evidence. The terrestrial meteorite flux consists mainly of ordinary chondrites, so we know that such undifferentiated bodies exist and may be common. Several of the S-type asteroids in our study have spectral parameters in Figure 4 which are consistent with those of known ordinary chondrites. This is especially true of 8 Flora, which is also the largest member of a dynamical family or group of families of about 200 asteroids which may have been formed by the collisional breakup of one or more larger bodies (Tedesco 1979). The asteroids in the Flora region are dynamically favored among main-belt asteroids as a source of meteorites (Wetherill and Williams 1979). Thus, the ordinary chondrites may be samples of some S-type asteroids in the main belt.

The discussion above shows that our spectroscopic data for S-type asteroids are consistent with the simple, undifferentiated model and with certain variations of the differentiated model. However, the differentiated models for S-type asteroids are not supported by meteoritic evidence, so we consider them improbable. On the basis of the available astronomical and meteoritic data, we therefore favor the conclusion that most S-type asteroids are undifferentiated bodies, similar to ordinary chondrites in composition.

We thank Michael J. Gaffey for many useful discussions and for the loan of meteorite samples, and Larry A. Lebofsky for photometric observations of our comparison stars. The LPL portion of the research was supported by NASA grants NSG 7607 and NSG 7070. The PSI portion of the research was supported by NASA contract NASW 3234. This is contribution No. 165 of the Planetary Science Institute, a division of Science Applications, Inc.

REFERENCES

Adams, J. B. 1974, *J. Geophys. Res.*, **79**, 4829–4836.
Affiattalab, F., and Wasson, J. T. 1980, *Geochim. Cosmochim. Acta*, **44**, 431–446.
Anders, E. 1964, *Space Sci. Rev.*, **3**, 583–714.
———. 1978, in *Asteroids: An Exploration Assessment*, NASA Conference Publication 2053, 57–74.
Chapman, C. R. 1976, *Geochim. Cosmochim. Acta*, **40**, 701–719.
Chapman, C. R., and Gaffey, M. J. 1979, in *Asteroids*, ed. T. Gehrels, (Tucson: University of Arizona Press), 655–687, 1064–1089.
Chapman, C. R., and Greenberg, R. 1981, *Lunar Planet. Sci.*, **12**, 129–131.
Chapman, C. R., Morrison, D., and Zellner, B. 1975, *Icarus*, **25**, 104–130.
Chapman, C. R., and Salisbury, J. W. 1973, *Icarus*, **19**, 507–522.
Drake, M. J. 1979, in *Asteroids*, ed. T. Gehrels, (Tucson: University of Arizona Press), 765–782.
Feierberg, M. A., Larson, H. P., Fink, U., and Smith, H. A. 1980, *Geochim. Cosmochim. Acta*, **44**, 513–524.
Gaffey, M. J. 1976, *J. Geophys. Res.*, **81**, 905–920.
Gaffey, M. J., and McCord, T. B. 1978, *Space Sci. Rev.*, **21**, 555–628.
Larson, H. P., and Fink, U. 1975, *Appl. Optics*, **14**, 2085–2095.
Larson, H. P., Fink, U., Treffers, R. R., and Gautier, T. N., III. 1976, *Icarus*, **28**, 95–103.
Lebofsky, L. A. 1980, private communication.
Low, F. J., and Rieke, G. H. 1974, in *Methods of Experimental Physics*, ed. N. Carleton, (New York: Academic), Vol. **12**, pt. A, 415–462.
McCord, T. B., and Chapman, C. R. 1975, *Ap. J.*, **197**, 781–790.
Pieters, C., Gaffey, M. J., Chapman, C. R., and McCord, T. B. 1976, *Icarus*, **28**, 105–115.
Remo, J. L., and Johnson, A. A. 1974, *Meteoritics*, **9**, 209–213.
Singer, R. B. 1981, *J. Geophys. Res.*, **86**, 7967–7982.
Sonett, C. P., and Reynolds, R. T. 1979, in *Asteroids*, ed. T. Gehrels, (Tucson: University of Arizona Press), 822–848.
Tedesco, E. F. 1979, *Icarus*, **40**, 375–382.
Veeder, G. J., Matson, D. L., and Smith, J. C. 1978, *A.J.*, **83**, 651–663.

Walker, D., Stolper, E. M., and Hays, J. F. 1979, in *Geochim. Cosmochim. Acta Suppl. 11, Proceedings of the Tenth Lunar and Planetary Science Conference*, Vol. **2**, *Early Solar System and Lunar Regolith*, 1995–2015.
Wasson, J. T., and Wetherill, G. W. 1979, in *Asteroids*, ed. T. Gehrels, (Tucson: University of Arizona Press), 926–974.
Wetherill, G. W., and Williams, J. G. 1979, in *Origin and Distribution of the Elements*, ed. L. H. Ahrens, (New York: Pergamon), 19–31.
Zellner, B. 1979, in *Asteroids*, ed. T. Gehrels, (Tucson: University of Arizona Press), 783–806.

CLARK R. CHAPMAN: Planetary Science Institute, 2030 East Speedway, Suite 201, Tucson, AZ 85719

MICHAEL A. FEIERBERG and HAROLD P. LARSON: Lunar and Planetary Laboratory, University of Arizona, Tucson, AZ 85721